# Resonant x-ray Raman scattering studies using synchrotron radiation

P. Eisenberger and P. M. Platzman
*Bell Laboratories, Murray Hill, New Jersey 07974*

H. Winick*
*Stanford University, Stanford, California 94305*
(Received 25 March 1975)

Synchrotron radiation is used to study resonant x-ray Raman scattering from copper metal. The study extends from above the $K$ absorption edge resonance to 500 eV below it.

Resonant Raman scattering in the visible is a technique which is undergoing a rapid growth as more tuneable lasers become available. Resonant Raman scattering in the x-ray region is theoretically expected, however its experimental presence has only recently been detected by Sparks.[1] He showed that the intensity of scattering varied from one material to another in a manner consistent with resonant enhancement due to the $K$ absorption edge approaching the fixed incident frequency. He was not able to study the resonant response of a single material, because of the lack of intense tuneable sources in the x-ray region. In this work synchrotron radiation is used to study, for the first time, the x-ray resonant Raman response of a single system, Cu metal, as the incident frequency is swept through the resonance condition.

The white, naturally collimated synchrotron radiation, which is two orders of magnitude brighter than the fixed emission lines from x-ray tubes and five to six orders of magnitude brighter than the bremsstrahlung emission from an x-ray tube, impinges upon a grooved silicon crystal (220 reflection $2d = 3.84$ Å) which functions as a monochromator, i.e., $\omega_1 = n\pi/d \sin\theta$, $\Delta\omega_1 = \omega_1 \cot\theta \delta\theta$. The quantity $\delta\theta$ is fixed by the slit size (1 mm) and distance from the source (22 m) to be 4.5 arcsec. The quantity $n$ is the order number indicating the possible presence of higher harmonics. In this experiment the intensity at the second harmonic was down by about three orders of magnitude. The monochromatized radiation is then incident on a copper sample inclined 45° to the beam. The scattered radiation is collected and energy analyzed at 90° from the incident beam direction by an intrinsic Ge detector which has a Gaussian resolution function with a sigma of 102 eV.

The experimental procedure was to fix the incident energy, collect the scattered radiation until sufficient statistics were accumulated, change the incident energy, and repeat the procedure. Since absolute energy calibration to better than a volt was fairly difficult to obtain in this experiment, the results are given relative to the absorption edge of Cu (see Fig. 1) measured by placing a thin Cu sample between two ion chambers and measuring the ratio of the incident to transmitted intensity as the incident energy was scanned in the absorption edge region.

The spectra taken using the solid-state detector with the incident energy far away from resonance were identical in shape to that previously observed by Sparks.[1] The spectra taken in the resonant region looked qualitatively like the resolution function but quantitatively varied in peak position, shape and intensity as one varied the incident energy with respect to the absorption edge.

In a typical electronic x-ray Raman process an x ray of frequency wave vector and polarization $(\omega_1, q_1, \epsilon_1)$ is scattered into the state $(\omega_2, q_2, \epsilon_2)$. The energy and momentum transferred in the pro-

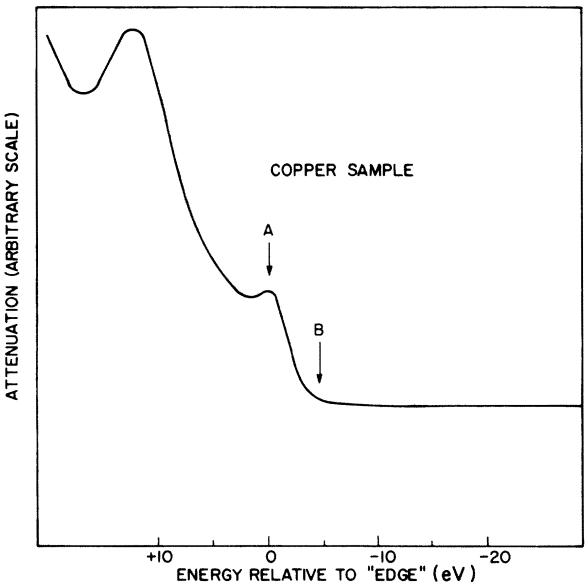


FIG. 1. Plot of the ratio transmitted to incident intensity for copper metal in the region of the $K$ absorption edge. This ratio is proportional to the attenuation. The zero of energy "the edge" corresponds to the break in the dispersion curve shown in Fig. 2.

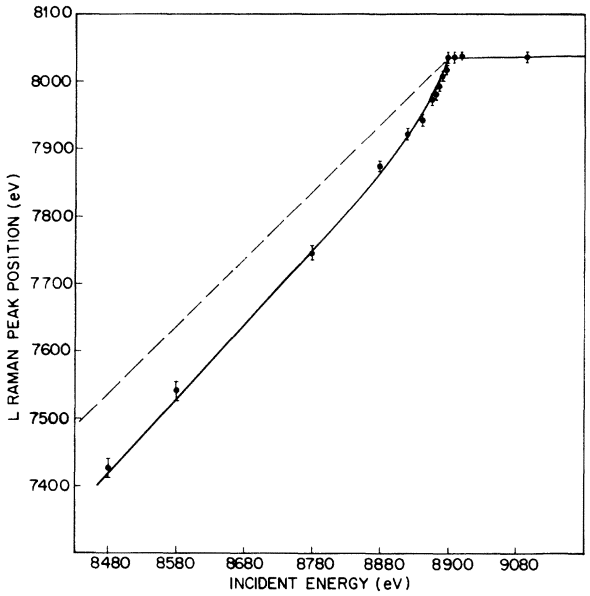


FIG. 2. Dependence of the peak position of the $L$ electron to continuum transition as the incident frequency $\omega_1$ is tuned in the region of the $K$ absorption edge. The solid line is the result of theoretical calculations using Eq. (5).

cess being given to an electronic excitation of the system. In this work we focus on the transitions which have a final state which has an $L$ hole and an additional electron in the continuum. For that transition we have summarized in Figs. 2 and 3 the results of our study for the dependence of the peak

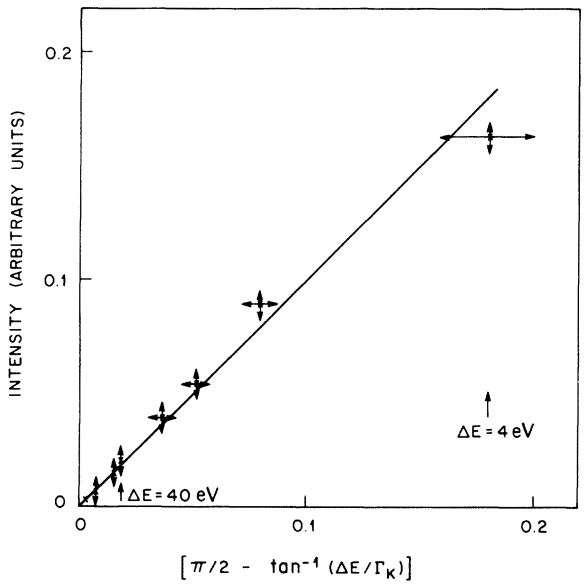


FIG. 3. Integrated intensity of the $L$ electron to continuum transition as the incident frequency $\omega_1$ is tuned in the region of the $K$ absorption edge. The solid line is Eq. (6).

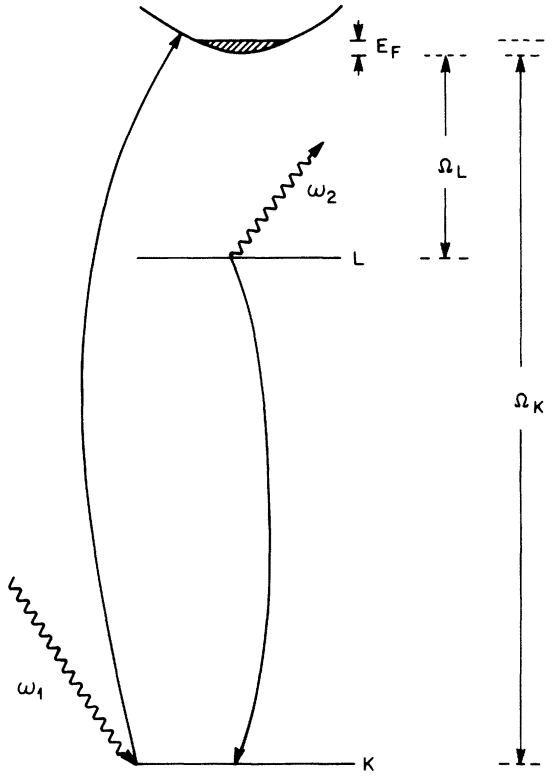


FIG. 4. Relevant energy levels for a simple metal.

position and the integrated intensity on the incident energy. The main observations we will want to discuss are the following: (i) The flatness and nonlinearity of the dispersion above and below the edge, respectively. (ii) Why the edge occurs where it does in metallic copper with respect to the attenuation curve shown in Fig. 1. (iii) The dependence of the integrated intensity on the energy difference of the input from the $K$ threshold.

The coupling of the x ray to the electrons is described by the usual nonrelativistic interaction Hamiltonian. To second order in the radiation field both $A^2$ and $\vec{p}\cdot\vec{A}$ terms contribute. In this experiment the polarization of the x rays from the synchrotron is such that $\vec{\epsilon}_1\cdot\vec{\epsilon}_2\simeq 0$ so that the $A^2$ term is negligibly small. Under suitable experimental conditions interference effects between those two terms can give important information.

The electronic process involved is shown schematically in Fig. 4. An electron is promoted to a $P$-like continuum state from the deep lying $K$ hole by the incoming photon. Another electron from the filled $L$ shell drops into the $K$ hole leaving a hole in the $L$ shell. The excited electron may be anywhere in the continuum. The spectrum of the outgoing radiation is continuous towards lower energy starting at a value, $\omega_2=\omega_1-(\Omega_L+E_F)$. The threshold for a real absorption process occurs

when $\omega_1 \geq \Omega_K + E_F$.

In addition to the simple one-electron transition depicted in Fig. 4 a number of important final-state effects can also be present: (i) The outgoing electron may scatter from its neighbors. (ii) The outgoing electron or hole may excite the Fermi sea leaving behind several electron-hole pairs, and the hole may interact with the excited electrons.

The first final-state effect modifies the matrix element for the absorption and leads to a modified form of *K-shell* extended x-ray absorption fine structure.[2] There is a real qualitative difference however. Since the $K$ hole in this Raman process is off the energy shell, the hole only gets a limited amount of time to detect the fact that the outgoing electron has scattered from its neighbors. As one tunes $\omega_1$ below the real absorption edge this time becomes shorter and the structure associated with such scattering should become weaker. Since the scale of extended x-ray absorption fine structure is only tens of volts we would not expect to see it in the current low resolution experiment.

The second set of effects give rise to modifications of the spectrum which are analogous to soft x-ray edge singularities which have been discussed in detail by several authors.[3] For the purpose of the current low-resolution experiment it is sufficient to analyze the process neglecting such many-body effects.

The one electron rate for scattering including only the resonant term is given by

$$\frac{dR(\omega_1,\omega_2)}{d\omega_2} = \left(\frac{\omega_2}{\omega_1}\right)\left(\frac{e^2}{mc^2}\right)^2 c \int \frac{d^3k}{(2\pi)^3} \times (1-n_{\vec{k}}) \left|M_{fi}\right|^2 \delta[\omega_1 - \omega_2 - (\epsilon_{\vec{k}} + \Omega_L)], \tag{1}$$

where

$$M_{fi} = \frac{\langle P|\vec{p}\cdot\vec{\epsilon}_2|S\rangle \langle k|\vec{p}\cdot\vec{\epsilon}_1|S\rangle}{m(\omega_1 - \epsilon_k - \Omega_K + i\Gamma_K)} . \tag{2}$$

The states $|S\rangle$ and $|P\rangle$ are one-electron atomic wave functions characterizing the bound $K$- (lifetime $\Gamma_K$) and $L$-shell electrons, respectively, while the state $|k\rangle$ and Fermi function $n_{\vec{k}}$ describe the conduction-electron wave function.

When the real part of the energy denominator in Eq. (2) vanishes (incident energy above threshold), the second-order process factors into an absorption followed by emission, e.i., ($K_\alpha$ characteristic lines)

$$R(\omega_1,\omega_2) = (\Gamma_K)^{-1} W^{\text{abs}}(\omega_1) W^{\text{emis}}(\omega_2), \tag{3}$$

with $\omega_2 = \Omega_K - \Omega_L$. Equation (3) simply states that the excited state of the system builds up at a rate $W$ and a time $(\Gamma_K)^{-1}$ where upon it fluoresces at a fixed frequency $\Omega_K - \Omega_L$. Above threshold Eq. (3) quite accurately describes the observed flatness of the spectrum.

The $K$ absorption threshold in metal is sharp since the density of states at the Fermi surface (threshold) is finite. Thus the break in Fig. 2 corresponds closely to the peak in Fig. 1 (see arrow $A$). In an insulator, because of the low density of states we would expect the break to occur somewhat sooner on the absorption curve, i.e., somewhat near arrow $B$ in Fig. 1.

Below threshold we may rewrite Eq. (1) as

$$\frac{dR(\omega_1,\omega_2)}{d\omega_2} = W^{\text{abs}}(\omega_1 - \omega_2 + \Omega_K - \Omega_L) \times \frac{\omega_2}{(\Omega_K - \Omega_L - \omega_2)^2 + \Gamma_K^2} . \tag{4}$$

Since the absorption rate depends solely on the $K$ absorption process it varies on an energy scale determined by the $K$-shell binding energy. In this experiment this means that it is slowly varying and may be evaluated at threshold, i.e., $W^{\text{abs}}(0)$. The frequency dependence which is present comes from the energy denominator in Eq. (4).

To obain the experimentally observed shape we convolve the resonance denominator with the experimental resolution function, i.e.,

$$\frac{dR(\omega_1,\omega_2)}{d\omega_2} = \frac{W^{\text{abs}}(0)}{(2\pi)^{1/2}\sigma} \int_0^{\omega_1 - \Omega_L + E_F} \frac{\omega'}{(\Omega_K - \Omega_L - \omega')^2 + \Gamma_K^2} \times \exp[-(\omega_2 - \omega')^2/2\sigma^2]. \tag{5}$$

The over-all intensity in the line is

$$I(\omega_1) \simeq W^{\text{abs}}(0)[(\Omega_K - \Omega_L)/\Gamma_K] \times [\tfrac{1}{2}\pi - \tan^{-1}(E_F + \Omega_K - \omega_1)/\Gamma_K]. \tag{6}$$

For $(E_F + \Omega_K - \omega_1)/\Gamma_K \gg 1$,

$$I(\omega_1) \simeq W^{\text{abs}}(0)(\Omega_K - \Omega_L)/(E_F + \Omega_K - \omega_1). \tag{7}$$

Equation (5) was used to generate theoretical spectra whose peak positions as a function of $\omega_1$ are plotted as a solid line in Fig. 2. The agreement between theory and experiment for the dispersion is very good. The nonlinear nature of the dispersion (i.e., $\Delta\omega_1 \neq \Delta\omega_2$) is caused by the effect of the finite resolution function on the changing shape of the resonant Raman transition as one moves away from resonance. The shape going from an essentially Lorentzian $K_\alpha$ emission lines at resonance to a sharp abosrption edge with a slowly falling intensity far from resonance. In Fig. 3 the measured area of the $L$ Raman transition is plotted as a function of $[\frac{1}{2}\pi - \tan^{-1}(E_F + \Omega_K - \omega_1)/\Gamma_K]$, where the data points were arbitrarily normalized and $\Gamma_K$ was chosen as 0.74 eV.[4] The solid line is the theoretically expected dependence and agrees quite well with the measured points.

With the limitations on resolution inherent in this study we see that the agreement between theory and experiment for the $L$ resonant Raman transi-

tion is very good. However, the importance of this study lies not so much in this agreement as it does in revealing that high-resolution studies will be possible with synchrotron radiation, which could provide additional information about absorption-edge phenomena and extended fine structure.[5] In addition, we should point out that these techniques need not be limited only to transitions involving the $L$ electrons but can also be used to study other more weakly bound electrons with the conduction electrons being of special interest.

ACKNOWLEDGMENT

Discussions with S. Doniach are greatly acknowledged.

---

*Research partly supported by the Stanford Synchrotron Radiation Project, NSF Grant No. GH 39525, in collaboration with the Stanford Linear Accelerator Center.

[1]C. J. Sparks, Jr., Phys. Rev. Lett. 33, 262 (1974).
[2]L. Azaroff, Rev. Mod. Phys. 35, 1012 (1963).
[3]P. Nozières and E. Abrahams, Phys. Rev. B 10, 3099 (1974).
[4]D. L. Walters and C. P. Bhalla, Phys. Rev. A 3, 1919 (1971).
[5]Y. B. Bannett and I. Freund, Phys. Rev. Lett. 34, 372 (1975